Dispersion and Reactivity of Supported Vanadium Oxide Catalysts

Komandur V.R. Chary
Catalysis Division, Indian Institute of Chemical Technology,
Hyderabad 500 007, India.

Abstract

A series of V_2O_5/Nb_2O_5 and V_2O_5/TiO_2 (anatase) catalysts with vanadia loading varying from 2-12 wt% were prepared and characterized by X-ray diffraction (XRD), temperature programmed reduction (TPR), electron spin resonance (ESR), BET surface area and oxygen chemisorption at 640 K. The catalytic properties have been evaluated for vapor phase ammoxidation of 3-picoline to nicotinonitrile. XRD results of V_2O_5/Nb_2O_5 catalysts suggest the formation of β-$(Nb,V)_2O_5$ phase at higher loadings. TPR profiles showed two peaks: the low temperature peak is due to reduction of surface vanadia species and the high temperature peak is due to reduction of Nb_2O_5. The oxygen uptake increases with increase of vanadia loading on niobia and titania, whereas the dispersion of vanadia decreases. The ammoxidation activity increases with vanadia loading up to 6 wt%, which corresponds to monolayer coverage and remains constant at higher vanadia loadings. The catalytic properties during ammoxidation of 3-picoline are related to the oxygen chemisorption sites.

Key words: vanadia-niobia, vanadia-titania catalysts, dispersion,3-picoline ammoxidation

Introduction

Supported vanadia catalysts are used in various industrial processes such as partial oxidation of benzene to maleic anhydride, O-xylene to phthalic anhydride, methane to oxygenates, ammoxidation of alkyl pyridines, and selective catalytic reduction of (SCR) of nitric oxide by ammonia [1-7]. The catalytic properties of the active vanadia phase can be greatly influenced by the nature of supported oxide and the dispersion of active component. The most commonly used supports for vanadia are Al_2O_3 [8-10], ZrO_2 [11,12], TiO_2 [13-15] and SiO_2. In recent years niobium-based materials have been employed as catalysts in numerous catalytic applications [16-26]. Niobia can be used as a support, as a promoter and as a unique solid acid. In addition to being used as a promoter, niobium oxide (Nb_2O_5) has also been used successfully as a support for the metal oxide catalysts [25]. The use of titanium dioxide as a catalyst support has several advantages over other classical supported oxides such as alumina and silica. One of the unique features of TiO_2 is, it interacts strongly with active phase of metal/metal oxide. TiO_2 exists in three crystallographic polymorphs viz., anatase, rutile and brookite. The anatase is a low temperature modification of titania and the phase transition to rutile generally occurs above 973 K. The vanadia supported on anatase TiO_2 is a classical example of support enhancement of active phase, especially if the vanadium oxide is applied on titania as a monomolecular layer. The optimal catalytic activity and selectivity are achieved when a one monolayer of vanadia is dispersed on anatase phase of TiO_2 [6,25]. Several studies have been reported in the recent past on the nature of vanadia species supported on alumina, silica, titania, and zirconia by employing an array of

complimentary spectroscopic methods such as laser Raman Spectroscopy (LRS) [29,30], ESCA [30,31,17], ESR [32,33], EXAFS [34,35], ^{51}V solid state NMR [8,36], low-energy ion scattering (LEIS), microcalorimetry [37], and diffuse reflectance fourier transform IR spectroscopy (DRIFTS) [38]. It is now evident that vanadium oxide remains as a highly dispersed amorphous monolayer phase containing isolated vanadium oxide species anchored to the support surface at low vanadia loadings on the support. However, at high vanadia loadings, the crystalline vanadia phase also co-exists with the monolayer phase.

In the present investigation we report the characterization of vanadium oxide catalysts supported on Nb_2O_5 and TiO_2 (anatase) by XRD, BET surface area, oxygen chemisorption, ESR and TPR measurements. We also report the differences in catalytic properties of these catalysts during the vapour phase ammoxidation of 3-picoline to nicotinonitrile. The purpose of this work is to estimate and compare the dispersion of vanadia supported on Nb_2O_5 and anatase TiO_2 and also to identify the changes in the structure of vanadium oxide species as a function of the active component loading.

Experimental Section

Vanadia supported catalysts were prepared by wet impregnation of Nb_2O_5 and TiO_2 with aqueous solutions of ammonium metavanadate to achieve 2-12 wt% V_2O_5 loadings in the finished catalysts. The supports used were Nb_2O_5 (surface area 55 m^2g^{-1}, CBMM Brazil HY-340), Anatase TiO_2 (surface area 92 m^2g^{-1}, Ti-Oxide UK Ltd.,). The impregnated samples were subsequently dried at 383 K for 16 h and calcined in air at 773 K for 6 h. Oxygen chemisorption was measured by static method using an all Pyrex glass system capable of attaining vacuum of 10^{-6} torr. The details of experimental set up are given elsewhere [8]. Prior to adsorption measurements the samples were prereduced in a flow of hydrogen (40 ml/min) at 640 K for 2 h. After reduction, the sample was evacuated at the same temperature for 1 h and oxygen adsorption uptakes was determined as the difference between the two successive adsorption isotherms measured at 640 K. BET surface area of the catalysts was determined by nitrogen physisorption at 77 K.

X-ray diffraction studies were carried out on Philips diffractometer using Ni-filtered Cu K_α radiation. ESR measurements were recorded at room temperature on a Bruker ER 200D-SRC X-band spectrometer with 100 kHz modulation. The reduced catalysts for ESR study were prepared in quartz tubes (25cms long, 4mm diameter), which formed part of the catalyst reduction apparatus. The reduction was carried out at 640 K for 2 h in a continuous flow (40ml/min) of low pressure purified hydrogen. The set up was subsequently evacuated for one hour at 10^{-6} torr. The catalyst thus prepared was transferred to the ESR sample tube and sealed off under vacuum. The unreduced samples were dried at 383 K for 16 h before ESR spectra was recorded at ambient temperature.

Temperature programmed reduction (TPR) experiments were conducted on Auto Chem 2910 (Micromertitics USA) instrument. The unit has a programmed furnace with a maximum operating temperature up to 1373 K. The instrument was connected to a computer which performs tasks such as

programmed heating and cooling cycles, continuous data recording, gas values switching, data storage and analysis. Prior to TPR studies the catalyst sample was pretreated at 673 K for 2 h in flowing hydrocarbon free dry air in order to eliminate the moisture and to ensure complete oxidation. After pretreatment the sample was cooled to room temperature. Carrier gas (5% hydrogen-95% argon) purified through oxy-trap and molecular sieves was allowed to pass over the sample. Temperature was increased from ambient to 1273 K at a heating rate of 10 K/min and the data was recorded simultaneously. The hydrogen consumption values are calculated using GRAMS/32 software.

A down flow fixed bed down flow reactor operating at atmospheric pressure and made of Pyrex glass was used for the catalysts testing during the ammoxidation of 3-picoline to nicotinonitrile. 2g of the catalyst diluted with equal amount of quartz grains were charged into the reactor and was supported on a glass wool bed. Prior to introducing the reactant 3-picoline with a syringe pump the catalyst was reduced at 673 K for 2 h in purified hydrogen flow (40 ml/min). After the prereduction, the reactor was fed with 3-picoline, ammonia and air keeping the mole ratio of 3-picoline: H_2O: NH_3: Air at 1:13:22:44 and contact time at 0.6 sec. The reaction was carried out at various temperatures ranging from 573 to 683 K. The liquid products obtained mainly nicotinonitrile were analyzed by HP 6890 gas chromatograph equipped with a Flame Ionization Detector (FID) using HP-5 capillary column. The carbon oxides were analyzed by HP-5973 GC-MS using a carbosieve column.

X -ray diffraction

The X-ray diffraction patterns of calcined samples of the V_2O_5/Nb_2O_5 catalysts are presented in Figure 1. At lower loadings only low temperature niobia phases are observed. The two low-temperature forms of Nb_2O_5, TT and T have long thought to be the same [39] due to their similar X-ray diffraction patterns. Also the TT phase does not always appear in pure components as starting materials. According to Ko and Weissman [29], the TT phase may be a crystalline form of T, stabilized by impurities.

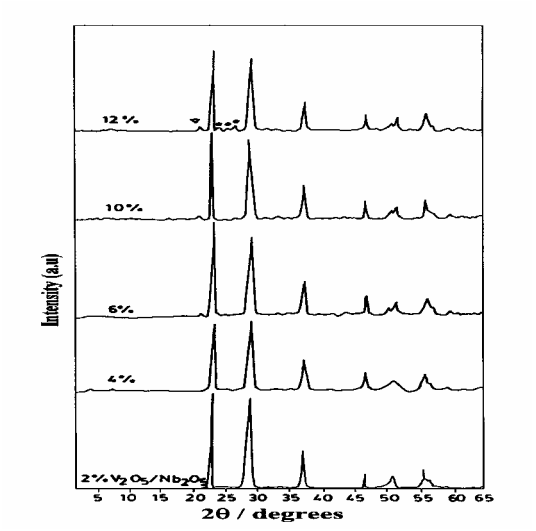

Figure 1: X-ray diffraction patterns of V_2O_5/Nb_2O_5 catalysts

Ko and Weissman [39] also reported that, samples calcined at low temperature (773 K) are X-ray amorphous. However, samples calcined between 773-873 K form TT-phase of Nb_2O_5, and samples calcined between 873-973 K favor the formation of the T-phase of Nb_2O_5. At 1073 K the M-phase forms and at 1273 K and above the H-phase of Nb_2O_5 is observed. In the present study the V_2O_5/Nb_2O_5 samples are calcined at 723 K, therefore we observe the TT-phase of Nb_2O_5. These XRD results are in agreement with the work of Smits et al. [40]. They also observed only TT-Nb_2O_5 phase for V_2O_5/Nb_2O_5 catalysts calcined at 823 K. However, the d-spacings of TT and T-phases of Nb_2O_5 are similar, but the intensity of d-spacings is different. At d = 3.94 Å (2θ = 22.5) the intensities are found to be 100 and 84 for TT and T-phases respectively and for the same phases at d=3.13 Å (2θ = 28.5) the intensities are found to be 90 and 100. It can be seen from Figure 1 that all the samples showed XRD peaks due to low temperature form of TT phase of Nb_2O_5 with an intense peaks at 2θ = 22.5 (100%) and 28.5 (90%). A mixed vanadium and niobium oxides such as β-$(Nb,V)_2O_5$ (JCPDS card No: 16-132) was formed at moderately high vanadia content and increases with further increase of vanadia content. This β-$(Nb,V)_2O_5$ phase can be observed with d = 3.77, 3.56, and 3.40 Å (2θ = 23.6, 25, and 26.19) for samples containing 10 and 12 wt% V_2O_5 supported on Nb_2O_5 shown with closed circles in Figure 1. The present results are in agreement with those of Gold Schmidt et al. [41], who proposed a structure similar to H-niobia. However, Watling et al [23] observed a β-$(Nb,V)_2O_5$ phase at 7 mol% of vanadia in their studies. Solid-state ^{51}V MAS NMR measurements [22] indicate that even in the case of samples in low vanadia (up to 7 mol%), vanadium exists in three different coordinations, i.e., in isolated tetrahedra, corner sharing dimeric tetrahedra and distorted octahedra. Thus, the present XRD results allow us to conclude to the formation of β-$(Nb,V)_2O_5$ phase, which contains isolated V tetrahedra. Wadsley and Andersson [42] reported that in this β-phase, vanadium replaces the niobium present in isolated tetrahedral sites at the junction of blocks of NbO_6 octahedra.

Powder X-ray diffraction patterns of V_2O_5/TiO_2 (anatase) catalysts are shown in Figure 2.

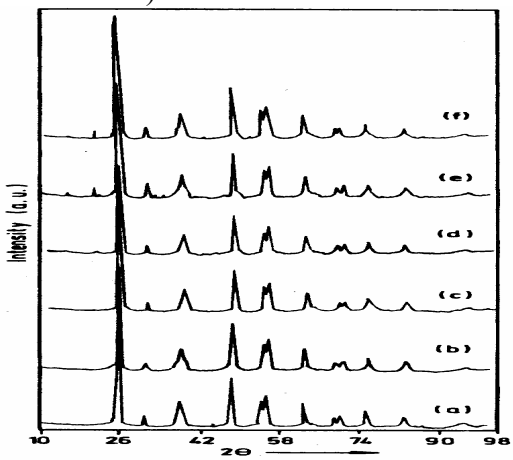

Figure 2: X-ray diffraction pattern of V_2O_5/TiO_2 (Anatase) catalysts (a) 2% V_2O_5/TiO_2 (b) 4% (c) 6% (d) 8% (e) 10% (f) 12%

It can be seen from Figure 2 that all the samples showed XRD reflections due to anatase TiO_2 with an intense peak at 2θ = 25.28 corresponding to diffraction by planes of (101) of TiO_2 (anatase). However, XRD peaks corresponding to V_2O_5 at 2θ = 20.2 can be seen only from 6 wt% samples in both the catalysts. The intensity of V_2O_5 diffraction line at 2θ = 20.2 increases with increase in vanadia loading. The absence of XRD peaks due to V_2O_5 at lower composition (below 6 wt%) indicates that vanadium oxide is present in a highly dispersed amorphous state on Nb_2O_5 and TiO_2 supports. However, at lower loadings of vanadia (<6 wt%) the possibility cannot be ruled out for the presence of vanadia crystallites having size less than 4 nm, which is beyond the detection capacity of the powder X-ray diffraction technique.

BET surface area and Oxygen chemisorption

The specific surface area and oxygen chemisorption values for V_2O_5/Nb_2O_5 and V_2O_5/TiO_2 catalyst samples are shown in Table 1 and Table 2 respectively. The other information such as oxygen atom site density, dispersion etc., derived from oxygen uptake were also given in Tables 1 & 2. The specific surface area of the catalysts was found to decrease sharply as a function of vanadia content. This decline of surface area with increasing vanadia loading might be due to blocking of the pores of the support by crystallites of vanadia.

Table 1: Results of oxygen uptake, dispersion, oxygen atom site density and surface areas of various V_2O_5/Nb_2O_5 catalysts

S. No	V_2O_5 loading on niobia wt%	Surface area m^2/g	O_2 uptake[A] μ moles/g	Oxygen atom site density (10^{18}) M^{-2}	Dispersion[B] O/V
1	2.0	50	86	2.1	0.78
2	4.0	49	156	3.8	0.71
3	6.0	47	223	5.7	0.68
4	8.0	44	259	7.1	0.59
5	10.0	44	303	8.3	0.55
6	12.0	44	330	8.6	0.50

[a]T (reduction) = T (adsorption) = 643 K

[b]Dispersion = fraction of vanadium atoms at the surface assuming $O_{ads}/V_{surf} = 1$

Figure 3 shows the oxygen uptake at 640 K for various V_2O_5/Nb_2O_5 and V_2O_5/TiO_2 catalysts plotted as a function of V_2O_5 content. The oxygen chemisorption capacities are found to increase with increasing the vanadia content implying that the dispersion decreases steadily with increase of vanadia content. Pure Nb_2O_5 and TiO_2 supports were also reduced under same conditions and the oxygen uptake of these oxides was found to be negligible. Vanadium oxide is present in well-dispersed state at low vanadia loadings on Nb_2O_5 and TiO_2 (Table 1 & 2). In both the series of catalysts the oxygen uptake values are found to increase with vanadia loading up to 6 wt% of V_2O_5 and levels off at higher vanadia loadings. The leveling off of oxygen uptake values at this composition of vanadia was attributed to the formation of V-oxide monolayer on niobia and titania supports. This loading corresponds closely to the theoretical monolayer capacity of vanadium oxide. From the unit cell dimensions of V_2O_5 an average value for a loading corresponding to a monolayer can be calculated as 1.2 mg

V_2O_5 per m^2 of the support. Bond et al. [43] reported, the weight concentration of V_2O_5 necessary to form a monolayer was 0.09 per m^2. Therefore, the theoretical monolayer capacity of V_2O_5 supported on niobia is found to be 4.95% and on anatase TiO_2 is about 8.28%.

Table 2: Results of oxygen uptake, dispersion, oxygen atom site density and surface areas of various V_2O_5/TiO_2 (Anatase) catalysts

S. No	V_2O_5 loading on titania wt%	Surface area m^2/g	O_2 uptake[A] μ moles/g	Oxygen atom site density (10^{18}) M^{-2}	Dispersion[B] O/V
1	2.0	65	107.4	1.99	0.98
2	4.0	60	187.0	3.75	0.85
3	6.0	58	267.7	5.56	0.81
4	8.0	62	315.3	6.13	0.72
5	10.0	58	363.1	7.54	0.66
6	12.0	53	362.3	8.23	0.55

[a]T (reduction) = T (adsorption) = 643 K

[b]Dispersion = fraction of vanadium atoms at the surface assuming $O_{ads}/V_{surf} = 1$

Thus, the saturation level of oxygen chemisorption might be attributed due to vanadia monolayer formation on niobia and titania supports. The leveling off of oxygen uptake at higher loadings could be due to presence of larger crystallites of vanadia phase as noticed in the XRD studies described earlier and this phase upon prereduction with hydrogen gas does not appreciably chemisorb oxygen. At low vanadia loadings, the uptake of oxygen approached the dashed line corresponding to a stoichiometry of one oxygen atom per vanadium atom. Using this stoichiometry Oyama et al. [44] defined the dispersion of vanadia as the fraction of total O atoms (determined from oxygen chemisorption uptake) to total V atoms in the sample. A substantial decrease of dispersion of vanadia is observed with increase of vanadia content in the catalyst samples. A comparison of vanadia dispersion on Nb_2O_5 and TiO_2 indicate that vanadia is well dispersed on anatase titania than niobia. The present oxygen chemisorption results are also further supported by the XRD results of these samples wherein, crystalline vanadia phase appears above 6% of V_2O_5 on various titania and niobia supports.

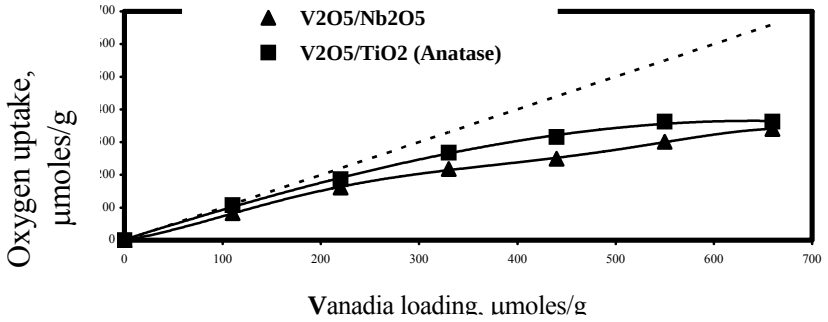

Fig 3: Oxygen uptake as a function of vanadia loading on niobia and titania ($T_{ads} = T_{red} =$ 640 K)

The temperature programmed reduction profile for bulk V_2O_5 is shown in Figure 4. It was found that bulk V_2O_5 exhibited multiple major reduction peaks when reduced with 5% H_2-in-Ar up to 1273 K. Koranne et al. [45] and Bosch et al. [46] have reported a similar observation; they have attributed this phenomenon to the following reduction sequence:

$V_2O_5 \rightarrow V_6O_{13} \rightarrow V_2O_4 \rightarrow V_2O_3$

The sharp peak at 965 K corresponds to the reduction of V_2O_5 to V_6O_{13} (first peak), the peak at 1003 K is associated with the reduction of V_6O_{13} to V_2O_4 (second step), and the peak at 1067 K corresponds to V_2O_3 formed by the reduction of V_2O_4. The reduction conditions applied were similar to those of the V_2O_5/Nb_2O_5 catalysts.

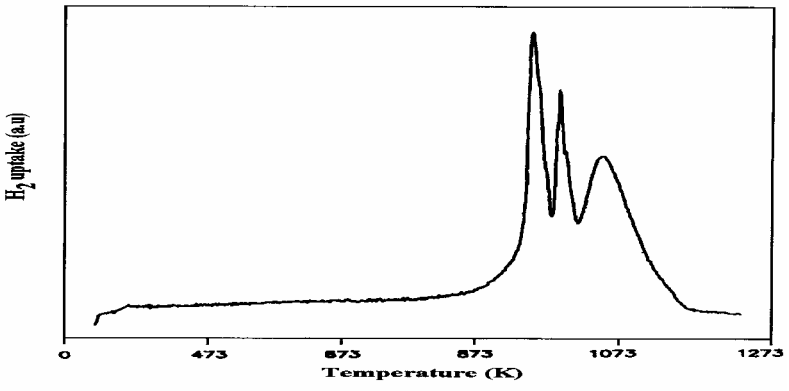

Figure 4: TPR profile of pure V_2O_5

TPR profiles of the vanadia supported on niobium oxide and titania catalysts are shown in Figures 5 & 6 respectively. The amount of hydrogen consumed during TPR for each peak is given in Table 3 & 4 respectively. In the V/Nb TPR profile, the first reduction peak is in the temperature range from 773 K to 973 K and is attributed to the reduction of vanadia. The second peak at higher temperature (1175 K and above) is due to niobia, whose peak position and hydrogen consumption values remained constant with increase in loading. The vanadia peaks could be identified from the profiles (though some of the peaks are very small humps): a low temperature peak at around 773 K, an intermediate temperature peak at ~873 K and third high temperature peak at around 955 K. These peaks are clearly visible at lower loading i.e., up to 6 wt% of vanadia on niobia. At higher loading, however, these peaks appear to merge into a single peak at 955 K. We attribute these low temperature peaks to the reduction of surface vanadia species. It is likely that the vanadia species becomes more polymeric in nature with an increase in vanadia loading, resulting in the merging of the low temperature peaks. The T_{max} values of the reduction of vanadia species were found to decrease with increase in loading up to 6 wt% and remained constant with further loadings. The shift in T_{max} to higher temperatures at higher loadings (above 6 wt%) is due to formation of β-$(Nb,V)_2O_5$ phase and/or due to the formation of crystalline V_2O_5. This clearly shows that the reducibility increased with loading up to 6 wt%.

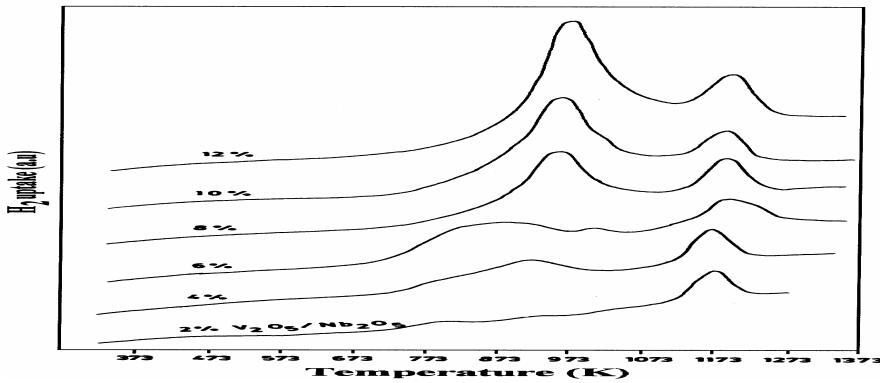

Figure 5: TPR profiles of V_2O_5/Nb_2O_5 catalysts

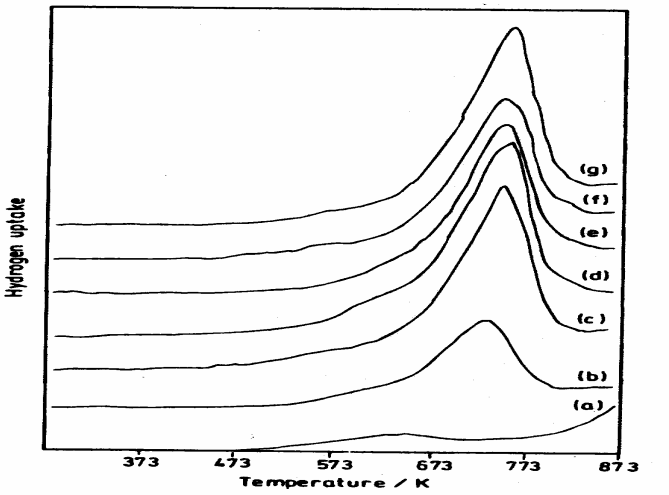

Figure 6: TPR profiles of V_2O_5/TiO_2 (Anatase) catalysts

In contrast, Roozeboom et al. [47] reported a two-stage reduction mechanism and attributed lower and higher temperature peaks as due to surface phases and crystalline V_2O_5, respectively.

Table 3 & 4: TPR results of various V_2O_5/Nb_2O_5 & V_2O_5/TiO_2 catalysts

S. No	wt% of V_2O_5 on Nb_2O_5	T_{red1} (K)	H_2 consumption (μmoles/g)	T_{red2} (K)	H_2 Consumption (μmoles/g)
1	2	932	80.3	1175	160.6
2	4	923	191.8	1193	160.6
3	6	892	312.3	1188	125.0
4	8	958	490.4	1186	165.0
5	10	952	727.0	1178	129.4
6	12	959	807.4	1195	165.0

S.No	wt% of V_2O_5 on titania	T_{max} (K)	Hydrogen consumption (μmoles/g)
1	2	717	46
2	4	735	87
3	6	742	96
4	8	740	85
5	10	739	70
6	12	741	89

The TPR profiles of V_2O_5/TiO_2 catalysts have shown (Figure 6) a single reduction peak. Baiker et al. also reported that titania supported vanadium oxide catalysts exhibited only a single reduction peak during TPR, if less than four layers of vanadium oxide was deposited. The reduction peak positions (T_{max}) reported in Table 3 show an increase of T_{max} values from 717 to 742 K with an increase of vanadia loading until a loading corresponding to 6% V_2O_5 was reached. Beyond 6 wt% V_2O_5 loading the T_{max} values did not change appreciably with an increase of vanaida loading in the sample due to the formation of vanadia crystallites. It is evident from Table 3 that vanadia is easily reducible on titania support than niobia support. It is also evidenced from oxygen chemisorption results that oxygen uptakes are higher in V/Nb catalysts than V/Nb catalysts. It has been observed that supported vanadium oxide catalysts reduce at much lower temperature than bulk vanadia and the reducibility of vanadia is strongly influenced by the kind of support used. The shift of T_{max} positions in TPR suggests that vanadia interacts strongly with titania (anatase) than niobia.

ESR technique was used to gain some information about the nature of vanadium species on niobia and titania supported vanadia catalysts. The ESR spectra of V_2O_5/Nb_2O_5 and V_2O_5/TiO_2 (anatase) catalysts recorded at 300K for the samples reduced in hydrogen are represented in Figures 7 and 8 respectively. Prior to the ESR measurements, the samples were reduced at 640K for 2h in hydrogen under identical conditions employed during the prereduction for oxygen chemisorption measurements. At low vanadia loadings the ESR spectra is well resolved with hyperfine splitting (hfs) due to ^{51}V (I=7/2). The analysis of ESR parameters suggests that the presence of V^{4+} in axial symmetry. The spectra of V_2O_5/TiO_2 samples are not well resolved to calculate ESR parameters. Unreduced samples show poorly resolved spectral features.

An examination of the ESR spectra of hydrogen-reduced catalysts suggests that the hyperfine structure diffuses at higher vanadia loadings and the spectra resemble that of singlet ESR spectrum of pure V_2O_5. The decrease of the intensity of ESR spectra with increase of vanadia loading in the catalyst samples is attributed to spin-spin coupling. The broadening of ESR spectra at higher loadings of vanadia might be due to presence of different surface vanadia species and probably due to crystalline vanadia as evidenced from XRD results reported earlier. Our ESR results are in agreement with the work of Inomata et al. [48]. According to Takahashi et al. [49] the agglomeration of V_2O_5 particles lead to an ESR spectrum of V^{4+} with diffuse hyperfine structure. The intense singlet peak for the reduced 10% V_2O_5/TiO_2 catalyst indicates agglomeration of V^{4+} ions in the reduced catalyst. The present ESR results further supports the dispersion measurements of oxygen chemisorption reported earlier. For example, a dispersion of 98% obtained for the catalyst having low vanadia loading (2% V_2O_5/TiO_2 anatase). This is in agreement with a well-resolved ESR spectrum due to ^{51}V and is obtained at this composition upon reduction of the sample under the experimental conditions employed for oxygen chemisorption.

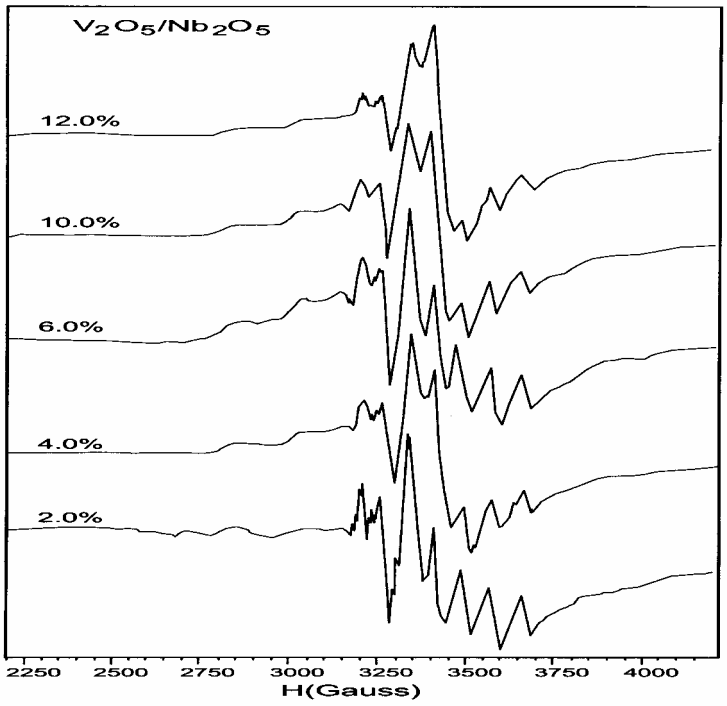

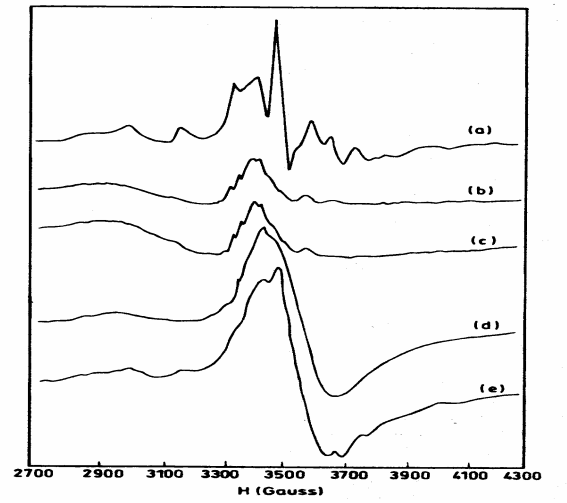

Figures 7 & 8: ESR spectra of V_2O_5/Nb_2O_5 and V_2O_5/TiO_2 catalysts
(a) 2% V_2O_5/TiO_2 (b) 4% (c) 6% (d) 8% (e) 10% (f) 12%

Ammoxidation of 3-picoline

The plot between V_2O_5 loading and conversion of 3-picoline (Figure 9) shows that conversion increases steadily up to 6 wt% V_2O_5 and remains constant above this loading. The activity of V_2O_5/TiO_2 catalysts is found to be higher than V_2O_5/Nb_2O_5 catalysts. Figure 10 shows the dependence of selectivity of nicotinonitrile formation on the vanadia loading supported on Nb_2O_5 and TiO_2. Both the series of catalysts are highly selective to nicotinonitrile formation. The higher activity of vanadia supported anatase TiO_2 can be explained based on the dispersion of vanadia determined by the oxygen chemisorption method.

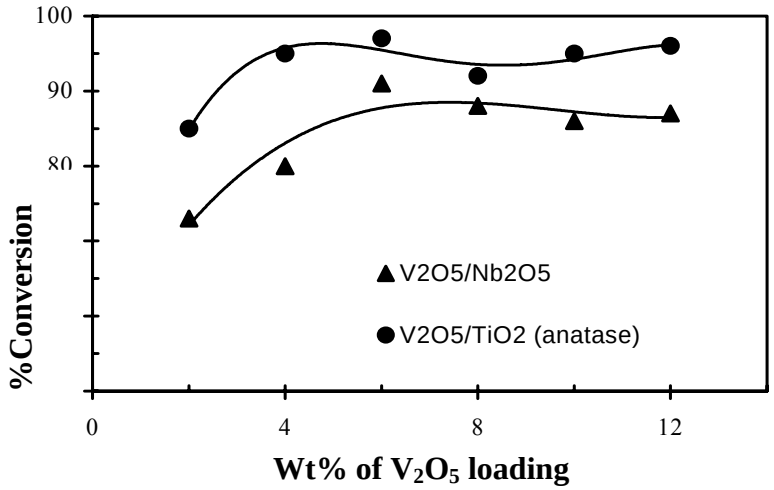

Figure 9: Ammoxidation of 3-picoline over V_2O_5/Nb_2O_5 and V_2O_5/TiO_2 catalysts

Oxygen chemisorption results of these catalysts suggest that vanadia disperses well on anatase than on the niobia. In our present study, the loading (6 wt%) corresponds closely to the theoretical monolayer capacity of vanadia supported on niobia and titania supports. Above 6 wt% vanadia loading the activity remains constant, suggesting the presence of same kind of vanadia species, probably due to the crystalline vanadia phase. According to Vejux and Courtine [50] the high activity of anatase polymorph of TiO_2 was ascribed due to their remarkable crystallographic fit between the (010) plane of V_2O_5 and the (010) and (001) plane of anatase TiO_2.

The conditions in the ammoxidation of 3-picoline are both reductive and oxidative, i.e., the hydrocarbons consume oxygen from the catalyst, which is then re-oxidized. It can be expected that under the steady state conditions the catalyst will contain a certain amount of lower oxides formed by reduction of the originally charged catalyst. The degree of reduction will depend on the reaction parameters. From EXAFS studies of low vanadia containing anatase Kozlowskii et al. [34] reported the existence of disordered vanadia species bonded to the titania surface via two bridging oxygen species. Additionally, there are two oxo-groups at each vanadia species. Several other authors concluded that anatase modifies the properties of vanadia by the formation of a stable monolayer of vanadia species directly bonded to the surface of the support [51,52].

Conclusions

The results of oxygen chemisorption results suggested that vanadium oxide is highly dispersed on anatase titania support than niobia. Oxygen chemisorption measured at 640K after the samples were prereduced at the same temperature provides a better method for determining the dispersion of vanadia. Dispersion of vanadia is found be high on anatase Titania support than on Nb_2O_5 support. XRD and ESR results further support the findings of oxygen chemisorption.

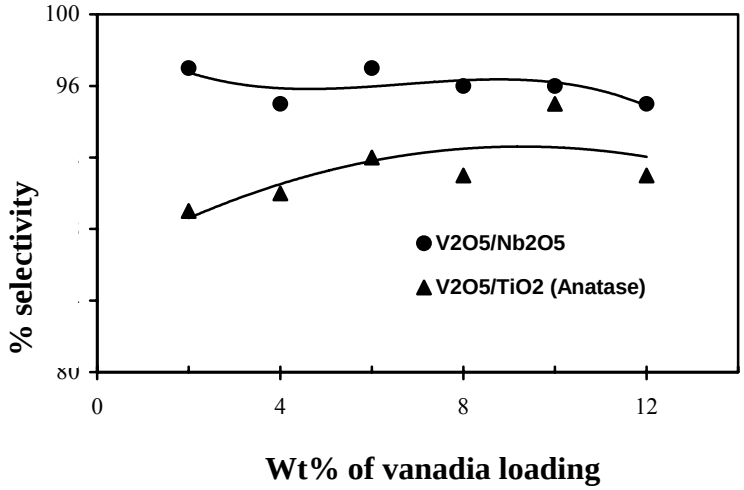

Figure 10: Dependence of selectivity of nicotinonitrile formation on V_2O_5/Nb_2O_5 and V_2O_5/TiO_2 catalysts

Conclusions

TPR results suggest that vanadia interacts strongly with TiO_2 anatase support than niobia. Vanadium oxide supported on anatase TiO_2 shows better catalytic activity in ammoxidation of 3-picoline than Nb_2O_5.

References

1.G. Deo, I.E. Wachs, J. Huber, *Crit.Rev.Surf.Chem*. 4 (1994**)** 1.
2.I.E. Wachs, B.M. Weckhuysen, *Appl.Catal.A: Gen*. 157 (1997) 69.
3.G.C. Bond, J. Sarkany, G.D. Parfitt, *J. Catal*. 57 (1979) 476.
4.C.R. Dias, M.F. Portela, G.C. Bond, *J. Catal*. 157 (1995) 344**.**
5.G.C. Bond, *Appl.Catal.A Gen*. 157 (1997) 91.
6.I.E. Wachs, R.Y. Saleh, S.S. Chan, C.C. Cherisch, *Appl.Catal.A: Gen*. 15 (1985) 339.
7.A. Baiker, M. Dollenmeir, A. Reller, *Appl.Catal.A: Gen*.35 (1987) 381.
8.K.V.R. Chary and G. Kishan, *J. Phys. Chem*. 99 (1995) 14424.
9.K.V.R. Chary, T. Bhaskar, K. Ramesh, J. Jyothi Maheshwar, V. Venkat Rao, *Appl. Catal*: *A Gen* 202(2000) 133.
10.N.K. Nag, K.V.R. Chary, B.M. Reddy, B. Rama Rao, V.S. Subra - hmanyam, *Appl. Catal*. 9 (1984) 225.
11.K.V.R.Chary, B.Rama Rao, V.S. Subrahmanyam,*Appl.Catal*.A74 (1991)1
12.K.V.R. Chary, K. Ramesh, G. Vidya Sagar, V. Venkat Rao, *J. Mol. Catal*. A : *Chemical* 198 (2003) 195.
13.K.V.R. Chary, *JCS Chem. Commn*. No.3 (1989) 104.
14.K.V.R. Chary, G. Kishan, T. Bhaskar, Ch. Shivaraj, *J. Phys. Chem*. No.3 (1998) 104.
15.K.V.R. Chary, G. Kishan, K. Srilakshmi, K. Ramesh, *Langmui*r 16 (2000) 7192.
16.K.V.R. Chary, G. Kishan, T. Bhaskar, *JCS Chem.Comm*un. No:15,(1999) 1399.
17.K.V.R. Chary, G. Kishan, Ch. Praveen Kumar, G. Vidya Sagar, J.W. Niemantsverdriet, *Appl. Catal A; Gen*. 245 (2003) 303.
18.K.V.R. Chary, G. Kishan, T. Bhaskar, K. Rajender Reddy, *J. Phys. Chem*. 105 (2001) 4392.

19.K.V.R. Chary, K. Rajender Reddy, T. Bhaskar, G. Vidya Sagar, *Green Chemistry* 4 (2002) 513.
20.K.V.R. Chary, K. Kalyana Seela, G. Vidya Sagar, B. Sridhar, *J. Phys. Chem*. (2004, In press).
21.K. Tanabe, *Catal. Today.* 8 (1990) 1.
22.R.H.H. Smits, K. Seshan, H. Leemreize, J.R.H. Ross, *Catal. Today*. 99 (1995) 9169.
23.T.C. Watling, G. Deo, K. Seshan, I.E. Wachs, J.A. Lercher, *Catal. Today*. 28 (1996) 139.
24.N. Ballarini, F. Cavani, C. Cortelli, C. Guinchi,P. Nobili, F. Trifiro, R. Catani, U. Cornaro, *Catal. Today* 78 (2003) 353.
25.J.M. Jehng, A.M. Turek, I.E. Wachs. *Appl. Catal*. A: *Gen* 83 (1992) 179.
26.I. Matsuura, H. Oda, K. Hoshida, *Catal. Today.* 16 (1993) 547.
27.M. Cherian, M. Someswara Rao, G. Deo, *Catal. Today* 78 (2003) 397.
28.G.C.Bond and K.Bruckman, *Faraday Discuss.Chem Soc*.72(1982**)** 235.
29.G.T. Went, L.J. Leu, A.T. Bell, *J. Catal*. 134 (1992) 479.
30.C.L. Pieck, S. del Val, M. Lopez Granados, M.A. Banares, J.L.G. Fierro, *Langmuir* 18 (2002) 2642.
31.N.K. Nag and F.E. Massoth, *J. Catal.* 124 (1990) 127.
32.K.V.R. Chary, B.M. Reddy, N.K. Nag, V.S. Subrahmanyam, C.S. Sunandana, *J.PhysChem*.88(1984) 2622.
33.V.K. Sharma, A. Wokaun, A. Baiker, *J. Phys. Chem*. 90 (1986) 2715.
34.R. Kozlowski, R.F. Pettifer, J.M. Thomas, *J. Phys. Chem*. 87 (1983) 5176.
35.T.Tanaka,H. Yamashita, R. Tsuchitani, T.Funabiki,S.Yoshida,*J.Chem.Soc*. *Faraday Trans.*1,84(1988) 2987.
36.H. Eckert and I.E. Wachs, *J. Phys. Chem.* 93 (1989) 6796.
37.J. Lebars, J.C. Vedrine, A. Auroux, S. Trautmann, M. Baerns, *Appl. Catal*. 119 (1994) 341.
38.A.W. Stobbe Kreemers, G.C. Van Leerdam, J.P. Jacobs, H.H. Brongersma, J.J.F. Scholten, *J. Catal*. 152 (1995) 130.
39.E.I. Ko, J.G. Weissman, *Catal. Today*. 8 (1990) 27.
40.R.H.H. Smits, K. Seshan, H. Leemreize, J.R.H. Ross, *Catal. Today* 16 (1993) 513.
41.H. Goldschmidt., *J. Metullurgia*. 62 (1960) 211.
42.A.D. Wadsley, S. Andersson, in "Perspectives in Structural Chemistry" (Dunitz, J. D. and Ibers, J. A. Eds.) Wiley, New York, 3 (1970) 19.
43.Bond, G.C.; Tahir, S.F. *Appl. Catal*. 199**1**, 71, 1.
44.S.T. Oyama, G.T. Went, K.B. Lewis, A.T. Bell, Somorjai, *J. Phys. Chem*. 93 (1989) 6786.
45.M.M. Koranne, J.G. Goodwin Jr. G. Marcelin, *J. Catal*. 148 (1994**)** 369.
46.H. Bosch, B.J. Kip, J.G. Van Ommen, P.J. Gellings, J.Chem. Soc., *FaradayTrans*. 80 (1984) 2479.
47.F. Roozeboom, M.C. Mittelmeijer-Hazeleger, J.A. Mouljin, J. Medema, V.H.J. de Beer, P.J. Gellings, *J. Phys. Chem*. 84 (1980) 2783.
48.M. Inomata, K. Mori, A. Miamoto, T. Ui, Y. Murakami, *J. Phys Chem*. 87 (1983) 754.
49.H.Takahashi, M. Shiotami, H. Kobayashi, J. Shoma, J. *J.Catal*. 14 (1969)134.
50.A. Vejux and J. Courtine, *J.Solid State Chem*. 23 (1978) 93.
51.G.C. Bond and S.F. Flamerz, *Appl.Catal*. 46 (1989) 89.
52. J. Haber, T. Machej, T. Czeppe, *Surf.Sci*. 15 (1985) 301.